Impact of Turbidity upon Iron Electrode based Electrocoagulation Pre-Treatment of Coal Seam Gas Associated Water

Syeda Nishat Ashraf, Jay Rajapakse, Les A. Dawes and *[1]Graeme J. Millar

School of Civil and Environmental Engineering & School of Mechanical, Medical and Process Engineering, Science and Engineering Faculty, Queensland University of Technology (QUT), Brisbane, Queensland, Australia.

The applicability of iron electrodes in an electrocoagulation (EC) process to treat coal seam gas (CSG) associated water comprising of high levels of turbidity (421 NTU) has been studied. The hypothesis was that the presence of turbidity may interfere with EC performance. Key objectives were to understand the influence of turbidity upon water quality when hydraulic retention time (HRT) and polarity reversal period (PRT) were tested. Extension of HRT promoted removal of dissolved alkaline earth ions (Ca 23 to 45 %; Mg 60 to 97 %; Ba 25 to 54 %; Sr 10 to 19 %), silicates (90 to 93 %) and boron (8 to 12.7 %); whereas turbidity was optimally reduced at a HRT value of 30 s (98.5 %). Turbidity particularly promoted magnesium removal which may be due to destabilization of the clay suspension. However, clay particles also inhibited the rate of floc settling. The greater performance of EC with increasing HRT was achieved at a cost of increased consumption of electrodes and electricity. PRT reduced power consumption with an optimal value being at least 5 min (4.12 to 3.88 kWh/kL for PRT values of 1 and 5 min, respectively). Removal rates of dissolved species were not greatly influenced by PRT or the presence of turbidity. Surface passivation at low PRT values produced higher amounts of hydrogen gas which caused the flocs to float. In summary, HRT, PRT, turbidity level and solution composition were critical parameters in relation to the potential use of EC in the CSG industry.

Key Words: Coal seam gas; coal bed methane; electrocoagulation; iron; associated water

*Corresponding author:
Graeme J. Millar | Professor
Science and Engineering Faculty | Queensland University of Technology
P Block, 7th Floor, Room 706, Gardens Point Campus, Brisbane, Qld 4000, Australia
ph (+61) 7 3138 2377 | email graeme.millar@qut.edu.au

1. Introduction

In the coal seam gas (CSG) industry, depressurization of the coal seams by extraction of water is required to release the entrapped gas [1]. Accordingly there are large volumes of associated water which may be used for applications such as crop irrigation [2]. The quality of CSG associated water depends upon the depth of the coal bed, the formation profiles of the coal and basin characteristics [3]. CSG associated water is saline in nature and the concentrations of the individual salts present are highly variable (total dissolved solids from hundreds to tens of thousands of mg/L) [4]. Nevertheless, sodium chloride and sodium bicarbonate species always comprise the major fraction of the impurities found in the CSG associated water [1, 2, 5, 6]. Salts of calcium, magnesium, barium, strontium, and iron in addition to dissolved silicates may be in lesser quantities, but they can be problematic in terms of their impact upon desalination technologies employed to make the water suitable for beneficial reuse [7, 8]. Another factor which impacts the performance of desalination methods for purification of CSG associated water is turbidity. Rebello *et al.* [9] analysed 150 CSG associated water samples from three different fields in the Surat basin for a range of water quality parameters. Notably, these authors reported that the total suspended solids (TSS) content varied between 5 and 7560 mg/L. The suspended solids probably comprised of a mixture of sand, silt, clay and other solids from bore operation [10].

Typically the associated water is not suitable for direct release to the environment [5, 11, 12]. Therefore, a range of technologies have been implemented to make the CSG associated water compliant with discharge and reuse regulations. One of the simplest strategies is to pH adjust the CSG associated water with acid and then to adjust the sodium adsorption ratio with micronized gypsum (to make it suitable for irrigation purposes). However, as shown by Vedelago and Millar [13] this process is limited to relatively low salinity CSG associated water to avoid inhibition of plant growth and degradation of soil quality. Ion exchange has also been employed for desalination of CSG associated water particularly in regions where the water is dominated by dissolved sodium bicarbonate species [14]. Use of a cation resin not only removed the sodium ions but also reduced solution alkalinity as the water became highly acidic under operating conditions. Alternatively, reverse osmosis (RO) is the most popular CSG associated water treatment method in Australia due to its proven performance for a range of water desalination applications [15].

However, as RO is a membrane based technique the challenge is always to minimize fouling by species such as sulphates/carbonates of alkaline earth ions, silicates, and organic matter [16-18]. Consequently, several pre-treatment methods have been implemented or considered for CSG associated water in order to stabilize performance of the central desalination stage [1]. Generally, pre-treatment technologies can be classified as coarse filtration, fine filtration, softening and chemical adjustment operations [1]. Coagulation using iron and aluminium based salts has been shown to remove some dissolved species such as alkaline earth ions and silicates under laboratory testing conditions using simulated CSG associated water samples [19, 20]. However, when real CSG associated water samples were evaluated the removal performance was inhibited by the presence of organic species. Le *et al.* [21] also described the application of a coarse disc filter as a coarse filtration stage prior to a microfiltration system prior to an RO unit used for CSG associated water desalination. As algae was also present in the CSG associated water several biocides were also added in the pre-treatment stage to protect downstream membranes and equipment from fouling.

Recently, electrocoagulation (EC) has been evaluated as an alternative method to chemical coagulation for CSG associated water treatment [22, 23]. Using aluminium electrodes, Millar *et al.* [22] found that alkaline earth ions and dissolved silicate species were significantly removed from the CSG associated water (>85 % effectiveness). Lesser amounts of dissolved organic carbon (<55 %), boron (<13.3 %) and fluoride (<44 %) were also removed by the EC process. Wellner *et al.* [23] also investigated the influence of CSG associated water composition upon the effectiveness of EC equipped with either aluminium or iron (mild steel) electrodes. Higher salt concentrations limited the reduction in alkaline earth ion content, whereas silicate removal was not significantly inhibited by solution salinity. Notably, iron electrodes were discovered to be less effective than aluminium electrodes for low and medium salinity CSG associated water samples; but potentially more effective at high salinity conditions. Iron based flocs were also recorded to settle faster than aluminium derived flocs which was an important issue with respect to practical operation of an EC system. Moreover, with aluminium electrodes the production of residual aluminium was found. This species may have a detrimental impact upon downstream membrane performance as precipitates may form which increase solution turbidity [24].

EC process optimization depends on critical factors such as hydraulic retention time (HRT), polarity reversal time (PRT), electrode characteristics, and current density. Xu *et al.* [25] found that the flow rate in the EC cell was critical in relation to removing copper from a salt solution. If the flow was too fast (*i.e.* short HRT value) the removal effectiveness was decreased. Alternatively, if the HRT value was too long then no significant gain in performance was recorded, yet inherently power/electrode consumption would be expected to increase per kL of water treated. Polarity reversal has been successfully employed by Timmes *et al.* [26] when using electrocoagulation to pre-treat seawater prior to an ultrafiltration stage. The fundamental premise was to alleviate issues associated with surface passivation of electrodes during EC operation which can increase the cost of power required. For example, Mao *et al.* [27] applied an alternating pulse current when treating a simulated wastewater with an EC unit equipped with aluminium electrodes. Up to 30 % energy reduction was stated for equivalent removal rates for chemical oxygen demand and notably the electrodes were discovered to wear more evenly. Iron (mild steel) and aluminium electrodes are the most common materials using in EC studies. Panikulam *et al.* [28] applied EC to remove kaolin turbidity from a sodium chloride solution and discovered that iron electrodes removed turbidity (> 95 %) in a wider pH range relative to Al electrodes. Pertinently, alkaline conditions were not conducive to turbidity reduction with aluminium electrodes; thus for CSG associated water samples which are normally pH >8, iron electrodes may be beneficial. Increasing current density is universally agreed to improve electrocoagulation performance as more floc is formed as the current density is increased [29].

This investigation addressed the research gap relating to the impact of hydraulic retention time and polarity reversal time upon the performance of an EC unit equipped with iron electrodes for CSG associated water pre-treatment. The hypothesis was that iron electrode performance during EC operation may not only remove multiple contaminants in CSG associated water but also be optimized by judicious choice of HRT and PRT. Research questions which were considered to support the hypothesis included: (1) What is the impact of HRT upon electrocoagulation performance when treating CSG associated water; (2) Which species are removed from the CSG associated water and to what extent? ; (3) What is the effect of turbidity on the removal of dissolved ions? (4) Does polarity reversal time influence

EC performance? To answer these research questions a bench top electrocoagulation unit was employed which was operated in continuous mode. Multiple iron (mild steel) electrodes were used in parallel and produced flocs were analysed for settling ability. A simulated coal seam gas water was treated which comprised mainly of sodium chloride and sodium bicarbonate species.

2. Materials and Methods

2.1 Electrocoagulation Tests

The benchtop electrocoagulation system consisted of a 1 L plexiglass cuboid vessel into which was placed 13 electrodes. Electrode plates were arranged in a parallel configuration with spacing of 0.3 cm between the plates. Each electrode was 15 cm (height) by 10 cm (width) by 0.3 cm (thickness). Only 24 faces were exposed during the EC process as two surfaces were attached to the side walls; thus the active anode area was 1800 cm^2. The EC cell was configured for vertical upflow of feed water which was delivered by a peristatic pump. A DC power supply equipped with a polarity reversal device was connected to the EC cell in a bipolar configuration. A pH probe and a conductivity probe were introduced at the outlet of the cell. A data logger was used to record the pH, conductivity, temperature of the effluent. The data logger also recorded the current supplied and corresponding voltage at a time resolution of 1 s.

Metal electrodes were cleaned with 3 % HCl solution and scrubbed lightly to remove all signs of greasy and loose particles from the surface. Subsequently, the electrode plates were kept in an oven overnight at 60°C. Prior to installation in the EC unit, each plate was weighed to allow calculation of mass consumed after testing. Electrodes were introduced into the EC cell and connected to the current supply in a bipolar configuration. Polarity reversal time and hydraulic retention time were fixed manually. Each experiment was continued for 40 min which was deemed to be sufficient to achieve stable operation [30].

2.2 Chemicals & Materials

All the chemicals used in this study were laboratory grade and supplied by Sigma-Aldrich and Chem-Supply Pty Ltd. The following salts were dissolved in deionized (DI) water with quantities calculated using an Excel spreadsheet model: H_3BO_3; $BaCl_2.2\ H_2O$; $CaCl_2.2\ H_2O$; KCl; $MgCl_2.6\ H_2O$; $NaSiO_3.5\ H_2O$; $SrCl_2.6\ H_2O$; NaCl; Na_2SiO_3; and $NaHCO_3$. Snobrite 55 kaolin clay was supplied by Unimin Australia and subsequently added to the simulated CSG associated water sample to introduce turbidity. Electrode materials were made of mild steel (<0.25 % carbon).

2.3 Simulated CSG Associated Water Sample

The required amount of each chemical was carefully weighed using a digital balance. Each chemical was initially added separately to deionised (DI) water under vigorous agitation in order to minimise problems with precipitation. All the solutions were then poured into a large graduated plastic drum of 140 L capacity. The required amount of kaolin was soaked in DI water for 30 minutes followed by manual stirring. The kaolin solution was then poured into the large drum. Finally, DI water was added until a final volume of 130 L was obtained. The resultant solution composition is shown in Table 1 and the final TDS was 5602 mg/L (which was regarded as a medium salinity CSG associated water sample [23]).

Table 1: Initial composition of simulated coal seam gas associated water

Species/Parameter	Value	Units
Sodium	1998	mg/L
Potassium	11.89	mg/L
Calcium	13.39	mg/L
Magnesium	10.03	mg/L
Barium	2.48	mg/L
Strontium	4.96	mg/L
Silicon	6.00	mg/L
Boron	16.91	mg/L
Chloride*	2452	mg/L
Bicarbonate	991.9	mg/L
Carbonate	89.6	mg/L
Solution pH	8.75	
Solution Conductivity	9112	microS/cm
Turbidity	421	NTU
True Colour	0	Pt-Co
Apparent Colour	1740	Pt-Co
Suspended Solids	600	mg/L
UV254	0.5	Abs

*Estimated based upon cation/anion balance of CSG associated water sample

2.4 Analysis Methods

2.4.1 Inductively Coupled Plasma - Optical Emission Spectroscopy (ICP-OES)

Dissolved ions (Na, K, Ca, Mg, Sr, Ba, B, & Si) were analysed by an inductively coupled plasma optical emission spectroscopy (Optima 8300 model Dual View ICP-OES spectrometer supplied by Perkin Elmer Company). The aqueous sample was filtered through 0.45 µm filters. Then the filtered solution was diluted by 2.5% nitric acid to adjust the pH to *ca.* 2. Samples were diluted to 1:10 and 1:100 ratio to compare the results using a Hamilton auto-diluter fitted with suitable syringes.

2.4.2 pH and Conductivity

Treated effluent pH and conductivity were recorded every second using TPS data logging software. A benchtop LABCHEM-CP meter and appropriate probes were supplied by TPS, Australia. The pH probe was calibrated using pH 4, 7 and 10 TPS calibration solutions. The probe was electrically grounded to avoid the interference of residual current. A conductivity probe with a k=10 sensor was used and calibrated with 58 mS/cm TPS calibration solution.

2.4.3 Apparent Colour/True Colour/ UV254

Apparent colour, true colour, and UV254 absorbance were measured using a UV-VIS spectrophotometer (Hach DR5000). Apparent colour and UV254 were measured for the unfiltered solution. Whereas, the solution was filtered through 0.45 µm syringe filters prior to recording true colour.

2.4.4 Turbidity

A portable turbidity meter of model Hach2100Q was used to measure the turbidity of the solution. Regular calibration of the instrument was performed using various turbidity standards.

2.4.5 Alkalinity

Carbonate and bicarbonate concentrations in the CSG associated water were calculated by titration using a standardized acid solution.

2.4.5 Optical Microscopy

To analyse the shape and colour of flocs optical microscopic images were captured using a Nikon Eclipse Ni upright microscope. Flocs were studied without any pre-treatment methodology such as drying in order to preserve physical features.

2.4.6 Floc Settling Rates

After completing the electrocoagulaiton test the solution was agitated to ensure uniformity and then poured into a 2L graduated cylinder. The height of the "mud line" was recorded as a function of settling time to determine the settling rate.

2.5 Electrode Consumption

Each electrode plate was weighed separately before and after the relevant electrocoagulation experiment. Plates were washed, oven dried overnight and cooled to the room temperature prior to weighing. The difference between before and after weights denoted the electrode consumption. Theoretical dissolution rate was calculated by using the Faraday equation [Equation 1].

Equation 1: $$\boldsymbol{m = {ItM}/{zF}}$$

Here, m is the mass of iron released to the solution (g), I is the average current applied through the experiment (A), t is the runtime (s), M is the atomic mass of iron (55.845 g/mol), z is the number of electrons transferred during anodic dissolution (=2) and F stands for Faraday's Constant (96,486 C/mol).

2.6 Power Consumption

Power consumed during the experiment was calculated by equation 2.

Equation 2: $$\mathbf{P = {IV}/{Q}}$$

Where P is the power consumed in Watt-h/L, I is the average current (A), V is the average voltage (V) and Q is the flow rate of influent (L/h).

3. Results and Discussion

3.1 Impact of Hydraulic Retention Time (HRT) upon Electrocoagulation Performance

Three different flow rates were examined which corresponded to hydraulic retention times of 20, 30, and 60 s for the CSG associated water. The aim of these tests was to evaluate the effect of HRT on the performance of an electrocoagulation unit equipped with iron electrodes for dissolved ions removal efficiency in presence of turbidity causing species.

3.1.1 Variation in Effluent pH and Turbidity of Treated CSG Water

Figure 1 shows the change in pH and turbidity level as a function of HRT.

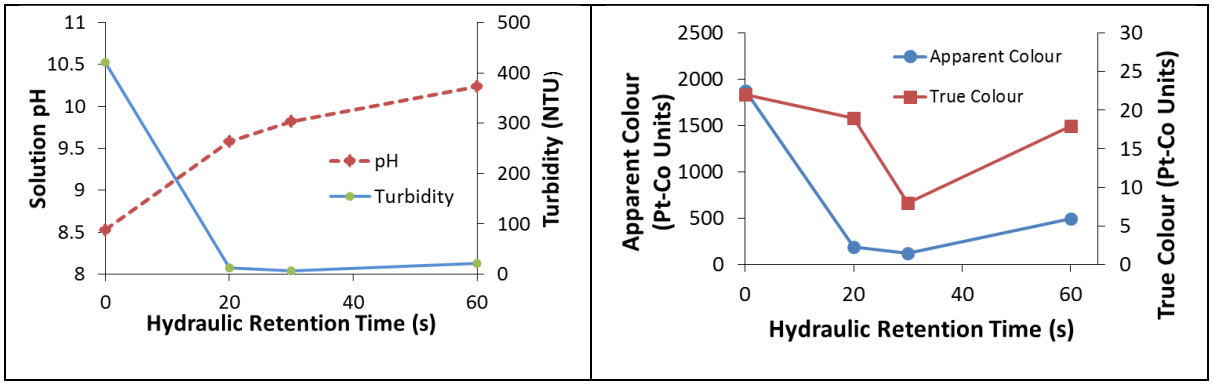

Figure 1: Impact of HRT upon effluent pH and turbidity of EC treated CSG associated water; PRT 3 min; test time 40 min

The final pH value was higher than the initial value and clearly depended upon the HRT value employed. The pH of the treated CSG associated water was raised to 9.58, 9.82, and 10.24 when HRT was 20, 30, and 60 s, respectively. Ciblak *et al.* [31] indicated that the rise in solution (up to pH 10.5) when iron was an anode in an EC cell was due to the dominance of the oxidation of iron metal to ferrous ions [Equation 3] and inhibition of the oxidation of water [Equation 4]. This conclusion was inferred from the considerably lower standard potential for dissolved ferrous iron production compared to that for water oxidation.

Equation 3: $$Fe^{o} \rightarrow Fe^{2+} + 2e^{-}$$

Equation 4: $$\mathbf{2\,H_2O \rightarrow 4\,H^+ + H_2 + 4\,e^-}$$

Thus, protons would not be available to neutralize hydroxyl ions produced at the cathode due to the process shown in Equation 5.

Equation 5: $$2\,H_2O + 2\,e^- \rightarrow 2\,OH^- + H_2$$

The highest turbidity reduction (98.5%) was achieved by 30 s HRT; albeit, an HRT value of 20 s was already sufficient to remove 97 % of turbidity from solution. Increasing HRT to 60 s induced a slight inhibition of turbidity reduction with 95 % removed under these conditions. The presence of suspended flocs in the solution may have been the cause of such turbidity (See Section 3.1.4]. Similarly, the apparent colour of the feedwater was 1880 Pt-Co units and this decreased to 188, 117, and 495 Pt-Co units for HRT values of 20, 30 and 60 s, respectively. Concomitantly, the true colour which was initially 22 Pt-Co units decreased to 19 and 8 Pt-Co units when HRT was 20 and 30 s, respectively. However, the true colour increased to 18 Pt-Co units for a retention time of 60 s. The apparent colour was the result of both iron compounds and kaolin particles suspended in solution. Whereas, the true colour measurements may reflect the presence of iron species in solution because the treated water was initially "green" in colour (Fe^{2+}) and this then turned to dark orange (Fe^{3+}) once the solution was removed from the reactor. During electrocoagulation with iron electrodes the primary dissolution of the anode proceeds *via* Equation 3 and then Fe^{2+} species can further oxidise to form Fe^{3+} ions as illustrated in Equation 6 [32].

Equation 6: $$\mathbf{Fe^{2+} \leftrightarrow Fe^{3+} + e^-}$$

Van Genuchten *et al.* [33] noted that the dissolved oxygen content of an iron electrode based EC cell was undetectable after electrocoagulation of arsenic contaminated groundwater. Upon exposing the treated solution to air the dissolved oxygen content returned to a similar value of the initial feedwater. Thus, oxidation of the Fe^{2+} ions to Fe^{3+} ions could proceed under aerobic conditions. During corrosion of iron the formation of "green rust" has also been reported. In solutions where there are bicarbonate/carbonate species present (such as is the case with CSG associated water) the iron hydroxyl carbonate of the general formula

$Fe_{x1}^{III}Fe_{x2}^{II}(OH)_{y1}(CO_3)_{z1}$ can be created [34]. Oxidation of this "green rust" material can also occur upon air exposure to form $Fe_{x1+x2}^{III}(OH)_y(CO_3)_z$. Further support for "green rust" was provided by Legrand *et al.* [35] who identified the presence of carbonate green rust $[Fe_4^{II}Fe_2^{III}(OH)_{12}]\ [CO_3.2H_2O]$ when they employed iron electrodes in a solution of sodium bicarbonate/carbonate. Legrand *et al.* [35] also discovered that the green rust oxidised when exposed to oxygen and in this case ferrihydrite was characterized.

From this interpretation of the behaviour of iron species in the electrocoagulation process a critical aspect was that the EC cell under operating conditions must have been anaerobic in character. The vigorous evolution of hydrogen bubbles at the cathode according to Equation 5 could displace the oxygen from the water sample. Dubrawski *et al.* [36] demonstrated that with various solutions of sodium sulphate, sodium chloride and sodium bicarbonate with iron electrodes that anaerobic conditions were indeed possible in the EC cell and that "Green Rust" was produced if carbonate was present.

3.1.2 Variation in Floc Mass and Electrode Consumption

Table 2 shows the change in floc mass and electrode consumption as a function of HRT. In general, as the residence time increased the floc mass produced and electrode mass consumed increased with increasing residence time of the CSG associated water in the EC cell. Power consumption per kL of water treated was also greater as HRT was extended. The ratios of floc mass to electrode mass lost were 1.64, 1.58, and 1.28 for HRT values of 20, 30 & 60 s, respectively. If we assume that the iron floc had the formula $Fe(OH)_2$ then the predicted mass ratio of floc produced to electrode loss would be 1.61. This latter calculation was in excellent agreement with the amount of floc determined when HRT was 20 & 30 s. However, there was a notably lesser quantity of floc measured for 60 s HRT compared to theoretical estimates. The experimental data also suggested that the presence of "green rust" was relatively minimal as the mass ratio of floc to iron consumed would be *ca.* 1.90 if this material dominated the floc composition (significantly higher than the recorded value of 1.28). Wei *et al.* [37] found that the formation of ferrite polymers was promoted at higher pH values when adding poly-ferric-acetate coagulant to wastewater containing kaolin and phosphate. If it was assumed that bridging Fe – $(OH)_2$ – Fe species were created [38], the ratio of floc to iron loss was calculated to be 1.30 which was very similar to the experimental value of 1.28. Hence, it

can be concluded that the iron species present in solution changed from monomeric to polymeric as the HRT was increased.

Table 2: Summary of experimental data CSG produced water was treated by electrocoagulation using iron electrodes and continuous run for 40 min (PRT 3 min)

HRT	**20 s**	**30 s**	**60 s**
Flow Rate (L/min)	1.66	1.16	0.60
Floc Mass (g/L)	1.71	2.29	3.89
Average Electrode Loss (g/L)	1.04	1.45	2.53
Theoretical Mass Loss (g/L)	1.15	1.67	2.97
Average Current (A)	9.17	9.28	8.54
Average Voltage (V)	31.81	30.61	27.97
Power consumption/Volume of Water Treated (kWh/kL)	2.93	4.08	6.63
Average Current Density (mA/cm^2)	5.09	5.15	4.74

In all cases the measured mass loss of the iron electrode was significantly lower than the mass predicted from the Faraday expression [Equation 1]. The discrepancy in electrode loss was calculated as 9.6, 13.2, & 14.8 % for HRT values of 20, 30 & 60 s, respectively. Typically, a super-Faradaic loss of metal from the anodes in an EC test has been described due to chemical dissolution of the surface [39, 40]. Dissolution of iron electrodes at a pH in excess of 9 typically produces soluble $Fe(OH)_4^-$ ions [41] (albeit, minimal dissolved iron was recorded in the treated effluent). However, competing with this process was the formation of carbonate species on the electrode surface which inhibited dissolution of iron ions and instead formed a passivated surface [42]. It is accepted that the less the degree of passivation (*i.e.* less resistance) of the electrode surface the greater the consumption of electrode occurs [43]. Increasing the HRT decreased the resistance of the iron electrode surface from 3.47 to 3.30 to 3.28 ohms for HRT values of 20, 30 & 60 s, respectively. Hence an explanation was required for why the cleanest electrode surface displayed the least mass loss. It was visually noted that a coating had formed on the electrode surface due to the EC tests. Timmes *et al.* [44] observed substantial accumulation of precipitate on the iron plates after pilot plant use which was consistent with the idea that passivation of the iron electrodes increased with time. van Genuchten *et al.* [45]

also found significant build-up of an oxide/hydroxide layer on iron electrodes used in the field for extended periods of time. Analysis suggested that the surface of the electrodes was majorly composed of a mixture of Fe_3O_4 and FeOOH. Therefore, although iron was lost from the anode to form the flocs, there was also an accumulation of a material such as iron carbonate or iron oxyhydroxide [46] which would explain the apparent net reduction in mass lost from the electrodes (balance between loss of iron and gain of carbonate or oxyhydroxide species).

3.1.3 Variation in Alkaline Earth Ions, Boron, and Silicates

All alkaline earth ions were reduced in concentration by application of electrocoagulation [Table 3]. Albeit, it was found that magnesium ions were preferentially removed from the CSG associated water (60.1, 81.7, and 96.9 % magnesium removal for HRT values of 20, 30, and 60 s, respectively).

Table 3: Concentration of dissolved species in CSG associated water before and after EC treatment; polarity reversal period 3 min; test time 40 min

		Hydraulic Retention Time (s)			
		0	20	30	60
Concentration (mg/L)	Mg	11.45	4.57 (60.1 %)	2.09 (81.7 %)	0.34 (97.O %)
	Ca	12.69	9.83 (22.6 %)	8.80 (30.7 %)	6.84 (46.1 %)
	Sr	5.18	4.66 (10.0 %)	4.53 (12.6 %)	4.19 (19.1 %)
	Ba	2.27	1.69 (25.3 %)	1.54 (32.2 %)	1.05 (53.8 %)
	B	18.37	16.91 (7.9 %)	16.3 (11.3 %)	15.71 (14.5 %)
	Si	8.31	0.84 (89.9 %)	0.66 (92.1 %)	0.56 (93.3 %)

The promotion of magnesium removal probably corresponded at least in part, to the raising of solution pH to 9.58, 9.82, and 10.24 as HRT values were increased from 20 to 60 s. Magnesium precipitation as brucite ($Mg(OH)_2$) is favoured by pH approaching 10 or greater [47]. Hafez *et al.* [48] recently found that magnesium ions were removed to a greater extent than calcium ions when using electrocoagulation to treat cooling tower blowdown water. However, no information was given regarding the mechanism which preferred removal of magnesium ions over calcium ions. Another factor may be the presence of the introduced solution turbidity, as previous studies of EC on CSG associated water without turbidity did not remove magnesium ions to the extent noted here (*ca.* 44.6 %) [23]. Sworska *et al.* [49] found

that under alkaline conditions the flocculation behaviour of syncrude tailings was markedly improved by the presence of magnesium ions. Mechanistically, it was proposed that the magnesium ions destabilized clay suspensions and allowed more rapid settling behaviour to occur. It thus appears that the interaction of the kaolin particles used to simulate solution turbidity in this investigation may have promoted removal of magnesium ions from the CSG associated water sample.

The solution pH in the range of 8.5 to 10.2 [Figure 1] should have been sufficient to precipitate calcium species as calcium carbonate. According to Malakootian *et al.* [50] a pH of 10 was very favorable in removing calcium (>97 %); a value which was significantly higher than the reduction in calcium ion concentration in this study (*ca.* 22.6 to 46.1 %). One explanation was the higher contact time (up to 60 minutes) used by Malakootian *et al.* [50] which would have been predicted based upon the current results to enhance calcium removal. In addition, CSG associated water is considerably more complex in terms of chemistry relative to the tap water sample tested by Malakootian *et al.* [50]. Indeed, Wellner *et al.* [23] found that calcium was reduced by only 24.9 % from CSG associated water similar to that described in this investigation. The presence of turbidity again may have promoted calcium ions removal relative to samples without clay addition. Sworska *et al.* [49] also indicated that calcium ions may interact with clay particles at high pH values. Hence, it is tentatively inferred that a similar process occurred in this study.

The relatively low percentage of strontium removed (10.0, 12.6 and 19.1 % at HRT values of 20, 30, and 60 s, respectively) was consistent with the established view that strontium removal was optimal at a pH of 7 to 8 [51]. In this study, the solution pH was from 9.58 to 10.24 after EC treatment which was not favorable for removal of strontium ions. Further inhibiting the removal of strontium ions was the fact that the initial strontium concentration was relatively low (5.48 mg/L); whereas concentrations up to 100 mg/L were reported as enhancing the percentage reduction in strontium present in solutions treated using EC [52]. In this study, the highest barium removal (53.8 %) was achieved for 60 s HRT. Notably, previous studies of CSG associated water treatment typically reported higher removal rates for barium ions (73.1 to 96.8 %) [23]; albeit, one must again consider the influence of varying CSG associated water composition and differences in physical properties such as pH.

Boron removal efficiency was not substantial in this study (7.9, 11.3, and 14.5 % for HRT of 20, 30, and 60 s, respectively). Widhiastuti *et al.* [53] achieved 70.3 % removal of boron using iron electrocoagulation to treat 10 mg/L boron in a sodium chloride solution. Notably the solution pH was only 8.5 which was considerably lower than the pH values in this study [Figure 1] and the residence time in the EC cell was 60 minutes. Notably the point of zero charge on the surface of the iron based sludge was pH 8.2. Hence, increasing the solution pH would result in a negatively charged surface which could be expected to repel negatively charged $B(OH)_4^-$ ions. Another factor responsible for lowering the effectiveness of EC for boron removal from CSG associated water was the relatively low concentration of boron species present. Sayiner *et al.* [54] demonstrated that the greater the boron concentration the higher the percentage of boron removed from solution by iron electrodes in an EC process. These authors examined solutions with up to 1000 mg/L which was substantially greater than the initial amount of 18 mg/L in this study. Hence, the relatively low EC performance for reduction of the amount of boron species in CSG associated water correlated with previous literature. In terms of the impact of HRT, Isa *et al.* [55] found that increasing the contact time of boron in an EC unit promoted the removal performance from *ca.* 75 % to greater than 95 %. Sorption studies suggested that the boron was bound to the flocs by a chemical bond and that intra-particle diffusion at least in part explained the rate limitations recorded.

Silica removal efficiency was excellent (89.9, 92.1, and 93.3 % at HRT of 20, 30, and 60 s, respectively). Den *et al.* [56] conducted a mechanistic study of silica removal from polishing wastewater by means of an electrocoagulation unit equipped with iron electrodes. It was concluded that silicate species were removed due to two possible processes. The first involved destabilization of the charge on the silicate species by Fe^{2+} ions liberated from the anode, thus allowing them to floc. The second mechanism was postulated to be enmeshment of silicates in iron oxide/hydroxide flocs. It appeared that the presence of clay particles did not inhibit the degree of silicate removal from the CSG associated water.

We note that irrespective of HRT iron was not present in a significant amount during any of our tests (*ca.* 0.02 mg/L). Mohora *et al.* [57] employed bipolar iron electrodes for EC treatment of arsenic in groundwater and they measured not only some residual iron species (< 0.5 mg/L) but also a distinct relationship to HRT. As the flow rate was increased (*i.e.* the

HRT decreased) the amount of residual iron present reduced. However, we note that Ciblak *et al.* [31] discovered that the identity of the electrolyte exerted a significant impact upon the electrode dissolution. Indeed, solutions with bicarbonate species present such as CSG associated water actually had essentially no residual iron in solution.

3.1.4 Floc Settling Behaviour and Characterization

Figure 2 shows the sedimentation rates of iron flocs produced during EC treatment as a function of HRT employed. In general, the higher the HRT value the slower the sedimentation rate measured. When extending the contact time of the fluid in the EC reactor the production of hydrogen gas from the cathodic oxidation of water can promote a floc flotation process [58]. Consequently, a correlation was evident between the increasing amount of gas evolved and the settling rate of the flocs produced.

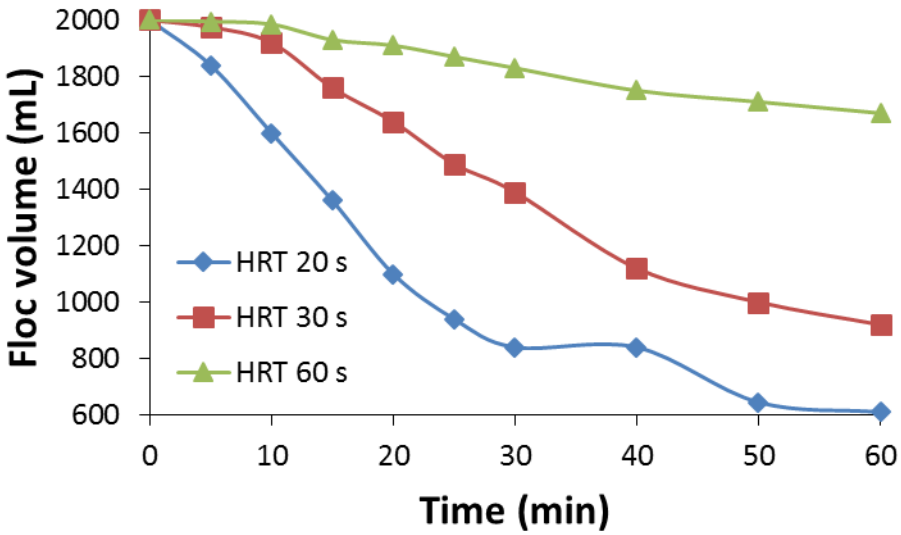

Figure 2: Floc sedimentation rate as a function of HRT; test time 40 min; PRT 3 min

In terms of practical application, Figure 2 suggested that a HRT value of 60 s may be problematic due to the slow settling rate recorded. This phenomenon was probably due to the greater production of hydrogen bubbles at the cathode during the EC process, as the contact time was increased. Wiley and Trent [59] described the effectives of an electrocoagulation/electro-flotation system for the clarification of surface water containing algae material. It was suggested that selection of the coagulant and hydrogen bubble concentration relative to suspended solids was a successful approach. Rojas *et al.* [60] further

noted that flotation was promoted by production of smaller bubble sizes which occurred under alkaline conditions. Hence, the observed settling behaviour of EC generated flocs in CSG associated water was consistent with previous literature. However, it was also observed that the settling rate when clay particles were present was surprisingly slower than when they were absent. For the 30 s HRT, after 1 h the settled volume of floc was *ca.* 920 mL, whereas when clay was absent the settled volume was *ca.* 450 mL [23].

In contrast, the removal rates of dissolved species were generally enhanced when HRT was increased from 20 to 60 s [Table 3]. Hence, a strategy to operate with 60 s HRT may be of practical interest if a means to accelerate the settling rate could be developed. One possible option to facilitate use of the extended HRT value, was use of a ballasted electrocoagulation process described by Brahmi *et al.* [61]. These authors added a combination of micro-sand and polyethyleneimine to enhance the settling properties of the flocs and noted a significant promotion of dissolved species removal could also be achieved by their approach.

Figure 3 illustrates the physical appearance of flocs produced during EC treatment at 20, 30 and 60 s HRT values, respectively. The flocs were orange-red in colour which inferred the presence of iron (III) oxides/hydroxides, a portion of which may have been formed from the oxidation of Fe (II) species by oxygen in air. Wellner *et al.* [23] characterized flocs from EC treatment of CSG associated water with iron electrodes and identified both magnetite (Fe_3O_4) and goethite (FeO(OH)). The CSG associated water was initially white in colour due to kaolin addition and turned dark green immediately after EC treatment. This dark green colour denoted the presence of iron (II) species. It was observed that the flocs were networked to each other and that the floc density increased as the HRT was extended. The presence of the kaolin particles captured by the flocs was also observed regardless of the HRT value applied (which was consistent with the data in Figure 1 that showed high turbidity removal at all contact times in the EC unit).

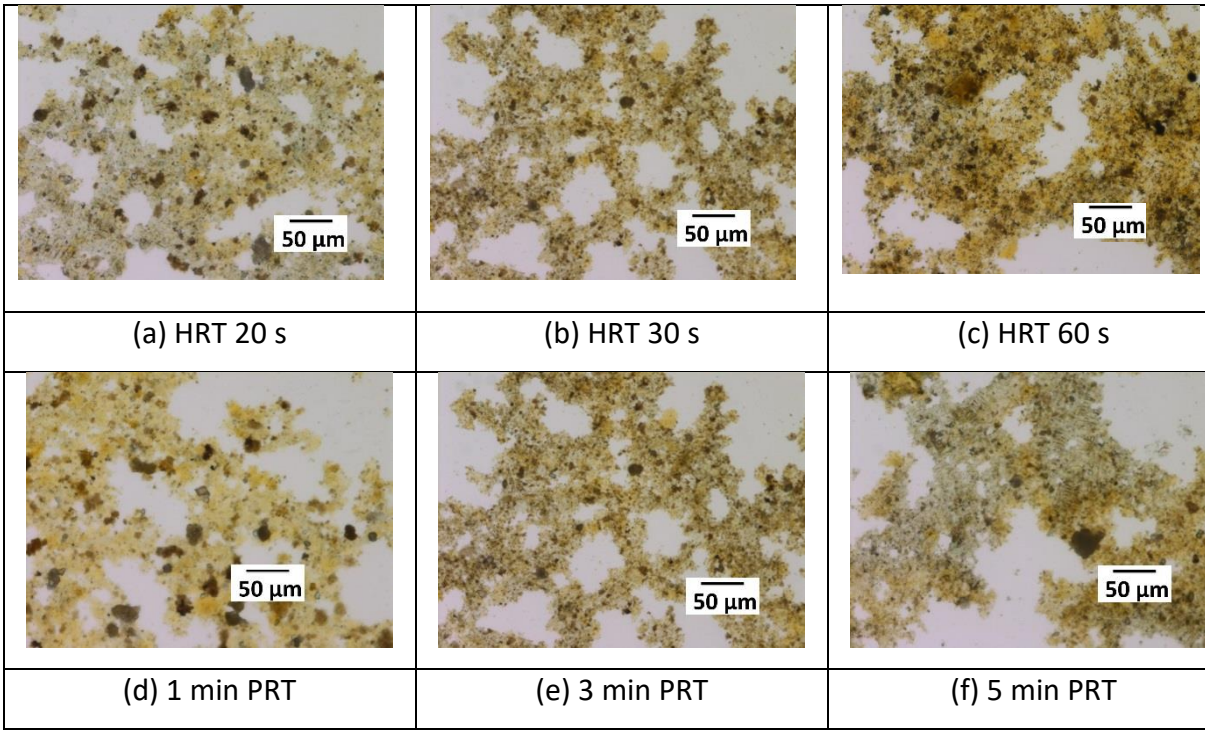

(a) HRT 20 s	(b) HRT 30 s	(c) HRT 60 s
(d) 1 min PRT	(e) 3 min PRT	(f) 5 min PRT

Figure 3: Optical microscopy images of flocs from electrocoagulation of different HRT values (a) 20 s, (b) 30 s & (c) 60 s (PRT = 3 min) and different PRT values (d) 1 min, (e) 3 min & (f) 5 min (HRT = 30s)

The optical images of the flocs supported the conclusion that greater gas production in the EC cell resulted in floatation of the flocs and inhibition of sedimentation. The denser flocs formed at 60 s HRT may have been expected to settle faster than those more porous flocs at 20 s HRT. As the opposite situation was the case floatation due to attachment of hydrogen bubbles was necessary to explain the settling behaviour illustrated in Figure 2.

3.2 Impact of Polarity Reversal Time (PRT) upon Electrocoagulation Performance

To evaluate the influence of PRT on EC performance experiments were conducted at three different PRT values, either 1, 3 or 5 min while the HRT value was constantly 30 s.

3.2.1 Variation in Effluent pH and Turbidity of Treated CSG water

Figure 4 shows the change in pH and turbidity as a function of PRT. It was observed that the solution pH increased during EC treatment compared to the initial pH of the CSG associated water (*c.f.* 8.55 to *ca.* 9.82). However, pH did not vary significantly whether PRT was 1, 3, or

5 min. Similarly, the effect of PRT on turbidity removal was negligible as >94.5 % reduction was recorded in all instances.

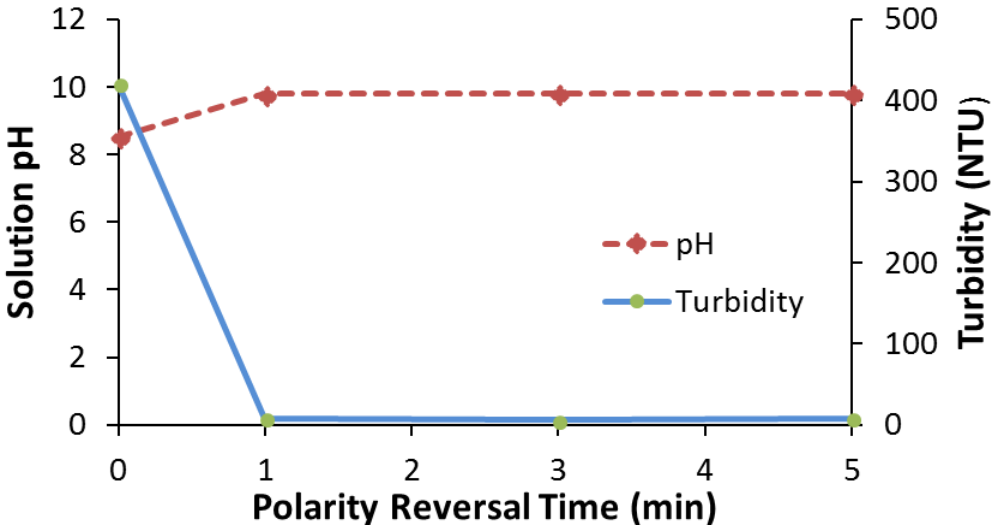

Figure 4: Impact of PRT upon effluent pH and turbidity of EC treated CSG water sample, HRT 30 s; test time 40 min

The ability of polarity reversal to influence turbidity removal has not been reported in published literature to the best of our knowledge. However, the data in Figure 4 indicated that PRT was not a major factor with respect to turbidity reduction in the EC unit.

3.2.2 Variation in Floc Mass, and Electrode & Power Consumption

Table 4 shows that the power consumption reduced gradually with the increase of PRT. Initially, power consumption was 4.12 kWh/kL for 1 min PRT and this diminished to 3.88 kWh/kL when PRT was increased to 5 min. As with the case when HRT was varied, the mass loss recorded of the electrode was less than predicted by the Faraday expression [Equation 1]. In this instance, the discrepancy in electrode amounts was 14.5, 13.2, & 5.7 % for PRT values of 1, 3, & 5 min respectively. Ciblak *et al.* [31] suggested that polarity reversal when using iron electrodes for electrocoagulation of saline solutions promoted the formation of reducing conditions in the EC unit. Hence, removal of passivating oxide/hydroxide films was accelerated. Pertile and Birriel [62] evaluated EC treatment of a wastewater solution from galvanic processing. Application of polarity reversal was found to increase the consumption of the electrodes used and this was again correlated with less oxide formation on the

electrode surface and greater pitting of the electrode material. Therefore, we can infer that the increasing PRT value decreased passivation of the electrode surfaces. The data also suggested that a PRT value in excess of 5 min may be beneficial as a balance between theoretical and recorded mass loss had not yet been achieved. Timmes *et al.* [44] discovered that the polarity reversal time when employed in an electrocoagulation pilot-plant for seawater treatment required the PRT be increased as the test time was lengthened. The basis of this variation in PRT was to ensure a constant dose rate for iron into the seawater. No mention of why the PRT value was required to be increased during the study by Timmes *et al.* [44] was given. However, the study of Fekete *et al.* [63] demonstrated that a certain minimum time was required for the de-passivation of electrode surfaces to occur when polarity reversal was applied during electrocoagulation. If the size of the passive layer increased then it is logical that the PRT required to remove the passivating oxide/hydroxide layer would also increase.

Table 4: Summary of experimental data of CSG water treated by EC equipped with Fe electrodes; HRT 30 s; test time 40 min.

PRT	PRT 1 min	PRT 3 min	PRT 5 min
Flow Rate (L/min)	1.17	1.16	1.16
Floc Mass (g/L)	2.26	2.29	2.30
Average Electrode Loss (g/L)	1.41	1.45	1.48
Theoretical Mass Loss (g/L)	1.65	1.67	1.57
Average Current (A)	9.28	9.28	8.71
Average Voltage (V)	31.2	30.61	30.98
Power consumption/Volume of Water Treated (kWh/kL)	4.12	4.08	3.88
Average Current Density (mA/cm^2)	5.15	5.15	4.84

3.2.3 Variation in Alkaline Earth Ions, Boron, and Silicates

Figure 5 presents the change in dissolved ions before and after EC treatment. Overall, it was observed that the removal of dissolved species was not substantially influenced by PRT. Application of a 3 min PRT was slightly superior in terms of EC performance with removal

rates of: magnesium (81.7 %); calcium (30.7 %); strontium (12.6 %); barium (32.3 %), boron (11.3 %) and silica (92.1 %).

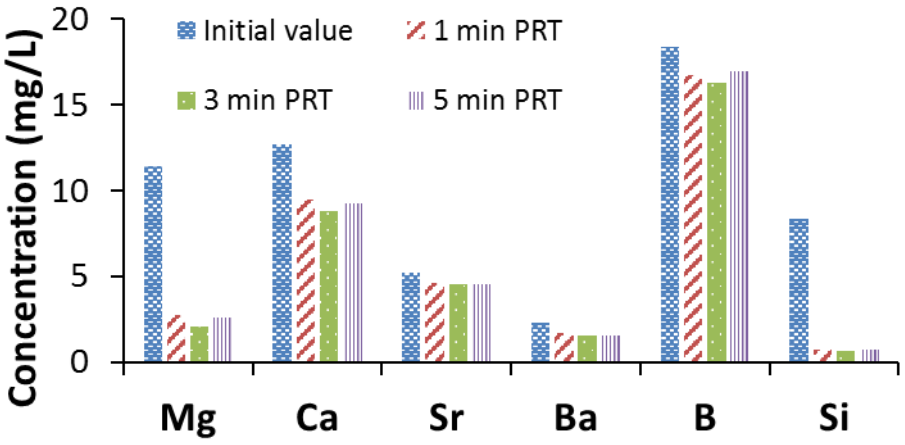

Figure 5: Concentration of dissolved species in CSG associated water before and after EC treatment as a function of PRT; test time 40 min; HRT 30 s

The relatively stable removal of the species outlined in Figure 5 as a function of PRT was not expected based upon the study of Pertile and Birrie [62]. These authors reported in excess of 20 % increase in the degree of removal of cyanide, zinc and nickel species from galvanic effluent which was attributed to the lesser passivation of the aluminium electrodes. From this data and that recorded in this study, the extent of the promotional effect of the polarity reversal period upon removal of dissolved species in solution can be inferred to relate to the degree of surface passivation present in that system. It would thus appear that the passivation of electrodes in this investigation was significantly less than that in the study of Pertile and Birrie [62]. This conclusion was in agreement with the study of Wellner *et al.* [30] which revealed that the overall salinity of a solution and identity of the salts present had a significant impact upon the passivation of the electrodes in an EC process. A point of interest was the fact that PRT 3 min appeared to be slightly better than PRT 5 min for reducing the concentration of the species denoted in Figure 5. From Table 4 the cleanest surface was created by using a PRT value of 5 min and this may have then be expected to give the highest removal performance. The reason for this behaviour has not been unequivocally resolved as yet.

3.2.4 Floc Settling Behaviour and Characterization

Figure 6 reveals the impact of PRT upon the sedimentation rates of EC produced flocs. There appeared to be a slight reduction in floc settling rate when a PRT value of 1 min was employed, whereas for 3 min and 5 min PRT the floc settling rate were similar.

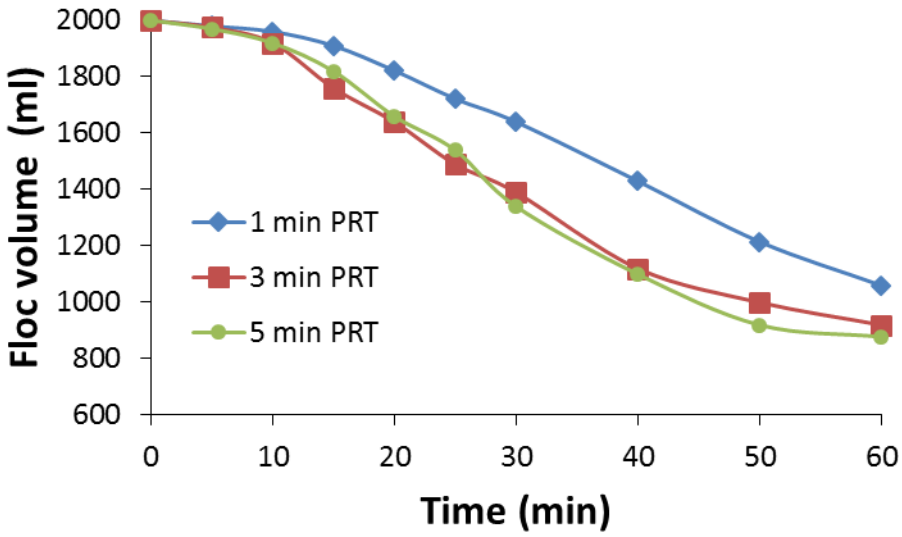

Figure 6: Floc sedimentation rate as a function of PRT: test time 40 min; HRT 30 s

When an anode is passivated this can promote the oxidation of water [Equation 4] which results in greater hydrogen production [30]. Thus, it can be postulated that the anode surface was most passivated at a PRT value of 1 min; as in this situation the excess hydrogen gas could "float" the produced flocs. This conclusion was in agreement with the data discussed in Table 4 wherein the power consumption was highest for a PRT value of 1 min.

Figure 3 (d)-(f) shows the optical microscopic images of flocs from EC treatment of the CSG associated water as a function of PRT. In general, the flocs all appeared to exhibit a network structure and evidence for entrapment of kaolin particles was observed. From the optical images it was difficult to ascertain any major differences in floc structure. Thus, the settling behaviour would be expected to be similar, apart from the importance of the quantity of hydrogen bubbles produced in the EC unit.

4. Conclusions

Electrocoagulation with mild steel (iron) electrodes has been demonstrated to be of interest for pre-treatment of CSG associated water. Solution turbidity and dissolved silicates were readily reduced by application of EC to very low residual levels. Alkaline earth ions which are known to potentially cause scaling problems with downstream equipment and membranes were also removed with magnesium being favoured.

Selection of appropriate hydraulic retention times was determined to exert a profound influence upon electrocoagulation performance when treating CSG associated water. Increasing HRT promoted the removal of dissolved alkaline earth ions, silicates, and boron. However, the corresponding substantial increase in electricity consumption may outweigh any performance gains. This is a matter for further techno-economic evaluation.

Polarity reversal time was found to be an important factor in relation to operation of an EC unit. Optimization of the PRT value could reduce surface passivation of the electrode surface and interestingly this value may be tailored to control the extent of anode dissolution. As the electrode surface became cleaner a slight, general improvement in removal performance of dissolved species in the CSG associated water could occur. In this instance, the PRT was required to be at least 5 min and it was recommended to explore longer timeframes in future studies.

The influence of turbidity in relation to EC treatment of CSG associated water has been demonstrated for the first time. The removal of dissolved species from the water sample was most impacted by the presence of turbidity. Moreover, HRT variation inherently was more impacted by the presence of turbidity compared to experiments where PRT was adjusted. As CSG associated water quality exhibits a wide range of turbidity values this parameter needs to be considered if practical implementation of EC is to be adopted.

5. Acknowledgements

We acknowledge provision of a scholarship for Syeda Nishat Ashraf (QUT Postgraduate Award (QUTPRA)). The Central Analytical Research Facility (CARF) at QUT is also thanked for access to the analytical facilities employed in this project.

6. References

[1] G.J. Millar, S.J. Couperthwaite, C.D. Moodliar, Strategies for the management and treatment of coal seam gas associated water, Renewable and Sustainable Energy Reviews, 57 (2016) 669-691.
[2] D. Monckton, J. Cavaye, N. Huth, S. Vink, Use of coal seam water for agriculture in Queensland, Australia, Water International, (2017) 1-19.
[3] C.A. Rebello, S.J. Couperthwaite, G.J. Millar, L.A. Dawes, Understanding coal seam gas associated water, regulations and strategies for treatment, Journal of Unconventional Oil and Gas Resources, 13 (2016) 32-43.
[4] I. Hamawand, T. Yusaf, S.G. Hamawand, Coal seam gas and associated water: A review paper, Renewable and Sustainable Energy Reviews, 22 (2013) 550-560.
[5] L.D. Nghiem, T. Ren, N. Aziz, I. Porter, G. Regmi, Treatment of coal seam gas produced water for beneficial use in australia: A review of best practices, Desalination and Water Treatment, 32 (2011) 316-323.
[6] G.J. Millar, S.J. Couperthwaite, S. Papworth, Ion exchange of sodium chloride and sodium bicarbonate solutions using strong acid cation resins in relation to coal seam water treatment, Journal of Water Process Engineering, 11 (2016) 60-67.
[7] S. Khan, G. Kordek, Coal seam gas: produced water and solids, Report commissioned for the independent review of coal seam gas activities in NSW by the NSW Chief Scientist & Engineer: School of Civil Environmental Engineering, The University of New South Wales, (2014).
[8] G.J. Millar, S. Papworth, S.J. Couperthwaite, Exploration of the fundamental equilibrium behaviour of calcium exchange with weak acid cation resins, Desalination, 351 (2014) 27-36.
[9] C.A. Rebello, S.J. Couperthwaite, G.J. Millar, L.A. Dawes, Coal seam water quality and the impact upon management strategies, Journal of Petroleum Science and Engineering, 150 (2017) 323-333.
[10] K.L. Hickenbottom, N.T. Hancock, N.R. Hutchings, E.W. Appleton, E.G. Beaudry, P. Xu, T.Y. Cath, Forward osmosis treatment of drilling mud and fracturing wastewater from oil and gas operations, Desalination, 312 (2013) 60-66.
[11] D. Mallants, J. Šimůnek, S. Torkzaban, Determining water quality requirements of coal seam gas produced water for sustainable irrigation, Agricultural Water Management, 189 (2017) 52-69.
[12] M. Stearns, J. Tindall, G. Cronin, M. Friedel, E. Bergquist, Effects of coal-bed methane discharge waters on the vegetation and soil ecosystem in Powder River Basin, Wyoming, Water, Air, & Soil Pollution, 168 (2005) 33-57.
[13] R. Vedelago, G.J. Millar, Process evaluation of treatment options for high alkalinity coal seam gas associated water, Journal of Water Process Engineering, 23 (2018) 195-206.
[14] R.S. Dennis, Continuous ion exchange for wyoming CBM produced-water purification: Proven experience, in: SPE E and P Environmental and Safety Conference 2007: Delivering Superior Environmental and Safety Performance, Proceedings, 2007, pp. 321-324.
[15] D. Blair, D.T. Alexander, S.J. Couperthwaite, M. Darestani, G.J. Millar, Enhanced water recovery in the coal seam gas industry using a dual reverse osmosis system, Environmental Science: Water Research and Technology, 3 (2017) 278-292.
[16] W. Den, C.-J. Wang, Removal of silica from brackish water by electrocoagulation pretreatment to prevent fouling of reverse osmosis membranes, Separation and Purification Technology, 59 (2008) 318-325.

[17] H.C. Duong, S. Gray, M. Duke, T.Y. Cath, L.D. Nghiem, Scaling control during membrane distillation of coal seam gas reverse osmosis brine, Journal of Membrane Science, 493 (2015) 673-682.
[18] K. Sadeddin, A. Naser, A. Firas, Removal of turbidity and suspended solids by electro-coagulation to improve feed water quality of reverse osmosis plant, Desalination, 268 (2011) 204-207.
[19] J. Lin, S.J. Couperthwaite, G.J. Millar, Applicability of iron based coagulants for pre-treatment of coal seam water, Journal of Environmental Chemical Engineering, 5 (2017) 1119-1132.
[20] J. Lin, S.J. Couperthwaite, G.J. Millar, Effectiveness of aluminium based coagulants for pre-treatment of coal seam water, Separation and Purification Technology, 177 (2017) 207-222.
[21] H. Le, Innovative commercial and technical solutions for CSG produced water treatment project, Chemical Engineering World, 52 (2017) 32-40.
[22] G.J. Millar, J. Lin, A. Arshad, S.J. Couperthwaite, Evaluation of electrocoagulation for the pre-treatment of coal seam water, Journal of Water Process Engineering, 4 (2014) 166-178.
[23] D.B. Wellner, S.J. Couperthwaite, G.J. Millar, The influence of coal seam water composition upon electrocoagulation performance prior to desalination, Journal of Environmental Chemical Engineering, 6 (2018) 1943-1956.
[24] R. Jiao, H. Xu, W. Xu, X. Yang, D. Wang, Influence of coagulation mechanisms on the residual aluminum - The roles of coagulant species and MW of organic matter, Journal of Hazardous Materials, 290 (2015) 16-25.
[25] T. Xu, X. Lei, B. Sun, G. Yu, Y. Zeng, Highly efficient and energy-conserved flocculation of copper in wastewater by pulse-alternating current, Environmental Science and Pollution Research, 24 (2017) 20577-20586.
[26] T.C. Timmes, H.C. Kim, B.A. Dempsey, Electrocoagulation pretreatment of seawater prior to ultrafiltration: Bench-scale applications for military water purification systems, Desalination, 249 (2009) 895-901.
[27] X. Mao, S. Hong, H. Zhu, H. Lin, L. Wei, F. Gan, Alternating pulse current in electrocoagulation for wastewater treatment to prevent the passivation of al electrode, Journal Wuhan University of Technology, Materials Science Edition, 23 (2008) 239-241.
[28] P.J. Panikulam, N. Yasri, E.P.L. Roberts, Electrocoagulation using an oscillating anode for kaolin removal, Journal of Environmental Chemical Engineering, 6 (2018) 2785-2793.
[29] L. Zaleschi, M.S. Secula, C. Teodosiu, C.S. Stan, I. Cretescu, Removal of rhodamine 6G from aqueous effluents by electrocoagulation in a batch reactor: Assessment of operational parameters and process mechanism, Water, Air, and Soil Pollution, 225 (2014).
[30] D.B. Wellner, S.J. Couperthwaite, G.J. Millar, Influence of operating parameters during electrocoagulation of sodium chloride and sodium bicarbonate solutions using aluminium electrodes, Journal of Water Process Engineering, 22 (2018) 13-26.
[31] A. Ciblak, X. Mao, I. Padilla, D. Vesper, I. Alshawabkeh, A.N. Alshawabkeh, Electrode effects on temporal changes in electrolyte pH and redox potential for water treatment, Journal of Environmental Science and Health - Part A Toxic/Hazardous Substances and Environmental Engineering, 47 (2012) 718-726.
[32] H.A. Moreno C, D.L. Cocke, J.A. Gromes, P. Morkovsky, J.R. Parga, E. Peterson, C. Garcia, Electrochemical reactions for electrocoagulation using iron electrodes, Industrial and Engineering Chemistry Research, 48 (2009) 2275-2282.

[33] C.M. Van Genuchten, S.E.A. Addy, J. Peña, A.J. Gadgil, Removing arsenic from synthetic groundwater with iron electrocoagulation: An Fe and As K-edge EXAFS study, Environmental Science and Technology, 46 (2012) 986-994.
[34] J.M. Blengino, M. Keddam, J.P. Labbe, L. Robbiola, Physico-chemical characterization of corrosion layers formed on iron in a sodium carbonate-bicarbonate containing environment, Corrosion Science, 37 (1995) 621-643.
[35] L. Legrand, G. Sagon, S. Lecomte, A. Chausse, R. Messina, A Raman and infrared study of a new carbonate green rust obtained by electrochemical way, Corrosion Science, 43 (2001) 1739-1749.
[36] K.L. Dubrawski, C.M. Van Genuchten, C. Delaire, S.E. Amrose, A.J. Gadgil, M. Mohseni, Production and transformation of mixed-valent nanoparticles generated by Fe(0) electrocoagulation, Environmental Science and Technology, 49 (2015) 2171-2179.
[37] Y. Wei, J. Lu, X. Dong, J. Hao, C. Yao, Coagulation performance of a novel poly-ferric-acetate (PFC) coagulant in phosphate-kaolin synthetic water treatment, Korean Journal of Chemical Engineering, 34 (2017) 2641-2647.
[38] G.J. Millar, A. Schot, S.J. Couperthwaite, A. Shilling, K. Nuttall, M. De Bruyn, Equilibrium and column studies of iron exchange with strong acid cation resin, Journal of Environmental Chemical Engineering, 3 (2015) 373-385.
[39] M. Mechelhoff, G.H. Kelsall, N.J.D. Graham, Super-faradaic charge yields for aluminium dissolution in neutral aqueous solutions, Chemical Engineering Science, 95 (2013) 353-359.
[40] M. Mechelhoff, G.H. Kelsall, N.J.D. Graham, Electrochemical behaviour of aluminium in electrocoagulation processes, Chemical Engineering Science, 95 (2013) 301-312.
[41] D.T. Moussa, M.H. El-Naas, M. Nasser, M.J. Al-Marri, A comprehensive review of electrocoagulation for water treatment: Potentials and challenges, Journal of Environmental Management, 186 (2017) 24-41.
[42] C.M. Van Genuchten, K.N. Dalby, M. Ceccato, S.L.S. Stipp, K. Dideriksen, Factors affecting the Faradaic efficiency of Fe(0) electrocoagulation, Journal of Environmental Chemical Engineering, 5 (2017) 4958-4968.
[43] H. Cesar Lopes Geraldino, J. Izabelle Simionato, T. Karoliny Formicoli de Souza Freitas, J. Carla Garcia, N. Evelázio de Souza, Evaluation of the electrode wear and the residual concentration of iron in a system of electrocoagulation, Desalination and Water Treatment, 57 (2016) 13377-13387.
[44] T.C. Timmes, H.C. Kim, B.A. Dempsey, Electrocoagulation pretreatment of seawater prior to ultrafiltration: Pilot-scale applications for military water purification systems, Desalination, 250 (2010) 6-13.
[45] C.M. van Genuchten, S.R.S. Bandaru, E. Surorova, S.E. Amrose, A.J. Gadgil, J. Peña, Formation of macroscopic surface layers on Fe(0) electrocoagulation electrodes during an extended field trial of arsenic treatment, Chemosphere, 153 (2016) 270-279.
[46] M. Reffass, R. Sabot, C. Savall, M. Jeannin, J. Creus, P. Refait, Localised corrosion of carbon steel in $NaHCO_3$/NaCl electrolytes: Role of Fe(II)-containing compounds, Corrosion Science, 48 (2006) 709-726.
[47] N. Esmaeilirad, K. Carlson, P. Omur Ozbek, Influence of softening sequencing on electrocoagulation treatment of produced water, Journal of Hazardous Materials, 283 (2015) 721-729.
[48] O.M. Hafez, M.A. Shoeib, M.A. El-Khateeb, H.I. Abdel-Shafy, A.O. Youssef, Removal of scale forming species from cooling tower blowdown water by electrocoagulation using different electrodes, Chemical Engineering Research and Design, 136 (2018) 347-357.

[49] A. Sworska, J.S. Laskowski, G. Cymerman, Flocculation of the Syncrude fine tailings Part I. Effect of pH, polymer dosage and Mg^{2+} and Ca^{2+} cations, International Journal of Mineral Processing, 60 (2000) 143-152.
[50] M. Malakootian, H.J. Mansoorian, M. Moosazadeh, Performance evaluation of electrocoagulation process using iron-rod electrodes for removing hardness from drinking water, Desalination, 255 (2010) 67-71.
[51] R. Kamaraj, S. Vasudevan, Evaluation of electrocoagulation process for the removal of strontium and cesium from aqueous solution, chemical engineering research and design, 93 (2015) 522-530.
[52] Z. Murthy, S. Parmar, Removal of strontium by electrocoagulation using stainless steel and aluminum electrodes, Desalination, 282 (2011) 63-67.
[53] F. Widhiastuti, J.Y. Lin, Y.J. Shih, Y.H. Huang, Electrocoagulation of boron by electrochemically co-precipitated spinel ferrites, Chemical Engineering Journal, 350 (2018) 893-901.
[54] G. Sayiner, F. Kandemirli, A. Dimoglo, Evaluation of boron removal by electrocoagulation using iron and aluminum electrodes, Desalination, 230 (2008) 205-212.
[55] M.H. Isa, E.H. Ezechi, Z. Ahmed, S.F. Magram, S.R.M. Kutty, Boron removal by electrocoagulation and recovery, Water Research, 51 (2014) 113-123.
[56] W. Den, C. Huang, H.C. Ke, Mechanistic study on the continuous flow electrocoagulation of silica nanoparticles from polishing wastewater, Industrial and Engineering Chemistry Research, 45 (2006) 3644-3651.
[57] E. Mohora, S. Rončević, J. Agbaba, K. Zrnić, A. Tubić, B. Dalmacija, Arsenic removal from groundwater by horizontal-flow continuous electrocoagulation (EC) as a standalone process, Journal of Environmental Chemical Engineering, 6 (2018) 512-519.
[58] M.M. Emamjomeh, M. Sivakumar, Review of pollutants removed by electrocoagulation and electrocoagulation/flotation processes, Journal of Environmental Management, 90 (2009) 1663-1679.
[59] P.E. Wiley, J.D. Trent, Clarification of algae-laden water using electrochemical processes, Water Science and Technology: Water Supply, 16 (2016) 314-323.
[60] R.H. Rojas, M.L. Torem, A.G. Merma, J.G.S. Puelles, H.J.B. Couto, Main factors affecting the size of hydrogen and oxygen bubbles produced in the electroflotation process, in: IMPC 2016 - 28th International Mineral Processing Congress, 2016.
[61] K. Brahmi, W. Bouguerra, S. Harbi, E. Elaloui, M. Loungou, B. Hamrouni, Treatment of heavy metal polluted industrial wastewater by a new water treatment process: ballasted electroflocculation, Journal of Hazardous Materials, 344 (2018) 968-980.
[62] T.S. Pertile, E.J. Birriel, Treatment of hydrocyanic galvanic effluent by electrocoagulation: Optimization of operating parameters using statistical techniques and a coupled polarity inverter, Korean Journal of Chemical Engineering, 34 (2017) 2631-2640.
[63] Ã. Fekete, B. Lengyel, T. Cserfalvi, T. Pajkossy, Electrochemical dissolution of aluminium in electrocoagulation experiments, Journal of Solid State Electrochemistry, 20 (2016) 3107-3114.